

**X. Delaune**

Commissariat à l'Energie Atomique,  
Département de Mécanique et de Technologie,  
91191 Gif/Yvette, France

**E. de Langre**

LadHyX, Ecole Polytechnique,  
91128 Palaiseau, France

**C. Phalippou**

Commissariat à l'Energie Atomique,  
Département de Mécanique et de Technologie,  
91191 Gif/Yvette, France

# A Probabilistic Approach to the Dynamics of Wear Tests

*Wear predictions of components belonging to pressurized water reactors require impact-sliding wear tests. Some scatter of the results have often been related to the complex dynamics of the test rig, which may be sensitive to small variations of parameters such as gaps or eccentricities. A probabilistic method is proposed here, which takes into account the actual dispersion of test parameters and the uncertainties on physical parameters for the computation of the test rig dynamics. The probability density function of wear work rate is used to assess the suitability of test parameters in terms of motion stability. An application of the method to some room temperature wear tests is presented.*  
[S0742-4787(00)02403-6]

## 1 Introduction

In pressurized water reactors, some flexible components such as controls rods or heat exchanger tubes are partially supported along their length. To facilitate assembly and allow for the thermal expansion, the support holes are made larger than the tubes. Flow-induced vibrations of tubes may cause impact-sliding motions against the supports and lead to wear of one or both of them [1,2].

In fact, it appears that the modeling of wear is complex owing to the large number of parameters involved in the wear process. For this reason, the most commonly used model in the context of impact-sliding tube dynamics, proposed by Frick et al. [3] and based on Archard's law [4], is defined by

$$\dot{V}(t) = k \cdot F_n(t) \cdot \dot{X}(t) = k \cdot \dot{W}(t), \quad (1)$$

where the wear rate,  $\dot{V}$ , or the volume loss rate, is related to a unique dynamic parameter named instantaneous wear work rate,  $\dot{W}$ . All physical aspects of wear are modeled in a wear coefficient,  $k$ . This coefficient is measured by wear tests performed on simulators (or wear test machines) where the vibratory motion is forced by mechanical excitation instead of fluid flow. The value of  $k$  is dependent on the materials of the two contacting bodies and the environmental conditions [3,5]. Moreover, it appears experimentally to depend on the vibratory motion of the tube, of which only the tangential velocity is taken into account in  $\dot{W}$ , whereas the wear process is not necessarily the same for all types of motion. For instance, as Frick et al. [3] have shown, Fig. 1, there may be a difference of two orders of magnitude between wear coefficients obtained from impact-sliding and pure fretting tests.

On the other hand, the question of reproducibility of such tests is rarely discussed in the open literature. By comparing the wear rate of identical tests executed on A.E.C.L. wear test rigs, Ko and Basista [6] showed that the ratios between extreme values may be about eight. In fact, they observed that the tube motion was initially unsteady and circular before settling down to a regular motion with impacts. They explain that if this change of motion persists long enough, the final mass loss will result from an average of at least two wear rates.

In practice, it should be noted that the undertaking of tests on rigs simulating pressurized water reactor environment is difficult and that the duration of these wear tests is typically of about several hundred hours. Therefore, a wear test is expensive, and it is thus of major importance to control its conditions.

The actual relationship between the control parameters and the actual dynamics of a wear test is complex and is, in practice, part

of the technical know-how. Our objective here is to develop a numerical approach of the dynamics of wear tests. Phalippou and Delaune [7] have shown that an accurate prediction of such dynamics was not possible due to the sensitivity of wear work rate to small variations of parameters such as the friction coefficient or the tube to support position. In that sense, a probabilistic approach is proposed here, following Payen and de Langre [8], who used a method based on Monte-Carlo simulation to take into account the uncertainties of physical parameters in the computation of the nonlinear vibrations of tubes under cross-flow.

The aim of this paper is to present a new method to help in the choice of wear test conditions. We show that by taking into account the actual scattering or uncertainties of test parameters in Monte-Carlo simulations, their practical suitability may be assessed.

## 2 Proposed Probabilistic Approach

**2.1 Computation of Wear Work Rate.** Wear work rate is actually a nonlinear function of input parameters  $X_i$ , which we shall write as

$$\dot{W} = G(X_1, X_2, \dots, X_n), \quad (2)$$

where  $G$  is not explicitly known, as nonlinear time-domain simulations of the tube dynamics are needed to obtain  $\dot{W}$ . The methodology used for the computation of the tube dynamics in the presence of impact-sliding motions is described in Rogers and Pick [9] and Axisa et al. [10]. The impact forces are computed with the use of an elastic impact force and a frictional force mod-

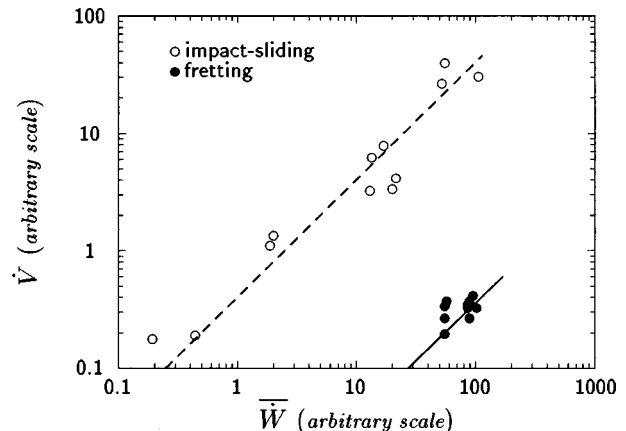


**Fig. 1 Comparison between impact-sliding and fretting wear coefficients (from Frick et al. [3])**

Contributed by the Tribology Division for publication in the ASME JOURNAL OF TRIBOLOGY. Manuscript received by the Tribology Division May 20, 1999; revised manuscript received February 24, 2000. Associate Technical Editor: J. A. Williams.

eled by Coulomb's law [11]. The time domain equations are projected on the modal basis of the system

$$m_n \ddot{q}_n + a_n \dot{q}_n + k_n q_n = f_e^n + f_i^n, \quad (3)$$

where  $m_n$ ,  $a_n$ , and  $k_n$  are the modal mass, the damping and the stiffness, respectively,  $q_n$  is the generalized displacement, the superimposed dot denotes time derivative and  $f_i^n$  and  $f_e^n$  are the modal projections of the impact and external forces. The set of Eqs. (3) is then integrated in time with the use of an explicit algorithm [10]. For our purpose, the tube motion is analyzed in terms of the mean value of the wear work rate which is defined by

$$\bar{W} = \frac{1}{T} \int_0^T F_n(t) \cdot |\dot{X}_i(t)| dt, \quad (4)$$

where  $T$  is a sufficient time duration to ensure that the computed nonlinear vibration is stationary. The number of modes needed in the modal basis is directly dependent on the impact stiffness,  $K_c$ . Experimental measurements of modal parameters, such as modal frequencies,  $f_n$ , shapes,  $\Phi_n$  and damping ratio,  $\xi_n$ , may be used to adjust the boundary conditions of the numerical model and, therefore, increase the accuracy of computation.

**2.2 Probabilistic Estimate of Wear Work Rate.** Equation (2) infers that if any parameter  $X_i$  is known through a probability density function (pdf), then the wear work rate also must be analyzed in terms of a pdf. The probabilistic approach considered here consists of computing the function,  $G$ , for  $M$  samples of random variables,  $X_i$ , each defined by a probability density function,  $p(X_i)$ . The choice of the variables,  $X_i$ , must be done among the set of parameters used in the numerical modeling. This includes the test parameters that are difficult to set or may vary during the test, such as the frequency of excitation, and the model parameters such as the friction coefficient, which is only an approximation of a complex reality.

For a given sample,  $j$ , of the set variables ( $X_1, X_2, \dots, X_n$ ), a nonlinear computation is carried out using the nonlinear deterministic computational techniques specified in the previous section.

Each computation yields a value of the mean wear work rate,  $\bar{W}_j$ . By repeating this for  $M$  samples, an estimate of the pdf of the mean wear work rate,  $p(\bar{W})$ , is derived. Moreover, if all sample calculations are saved, one can access each and every set of variables and their corresponding effect on work rate.

**2.3 Use of Probabilistic Results.** The criteria, proposed here to evaluate the suitability of test parameters, is based on analysis of the resulting pdf of the mean wear work rate,  $p(\bar{W})$ . As stated before, it is important in practice that the actual mean wear work rate in a given test is not significantly different from that expected. Therefore, one can understand that a pdf which is well centered around a mean value means that the actual wear work rate stays close to this mean value. Conversely, an ill-shaped pdf allows several ranges of wear work rate to possibly exist. In the next section, a situation is shown which is not acceptable in practice. Indeed, this might lead to either a test that runs at a value of mean wear work rate significantly different from that expected or a test where the mean wear work rate changes.

### 3 Application to a Room Temperature Wear Test Rig

**3.1 Description of the Wear Test Rig.** In the application considered here, we shall use a room temperature wear test machine which can operate in air or in water. This machine (Fig. 2) has been designed by the Atomic Energy Canada Limited (A.E.C.L.) [9,12–14] to provide a simple unidirectional tube motion, or a combined impact and sliding motion depending on the test parameters. It consists of a cantilever tube excited by a vibration generator attached to its free end. The tube wear specimen, mounted on the excitation tube, may vibrate against an annular support wear specimen, which is held by four piezo-electric force

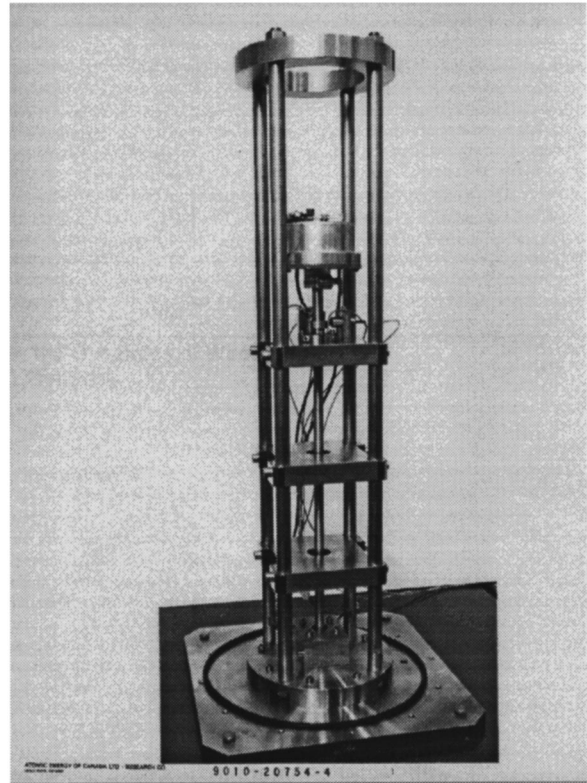


Fig. 2 Room temperature wear test rig (from A.E.C.L.)

transducers preloaded and equally spaced around the circumference. These transducers measure the dynamic interaction between the tube and the support. A more detailed description of the technique used to measure these forces may be found in Fisher and Ingham's paper [15]. Relative motions are measured using a pair of eddy-current displacement probes located in a plane above the force transducers.

The vibration generator, as shown in scheme Fig. 3, consists of two stepper motors with eccentric masses. A control unit makes

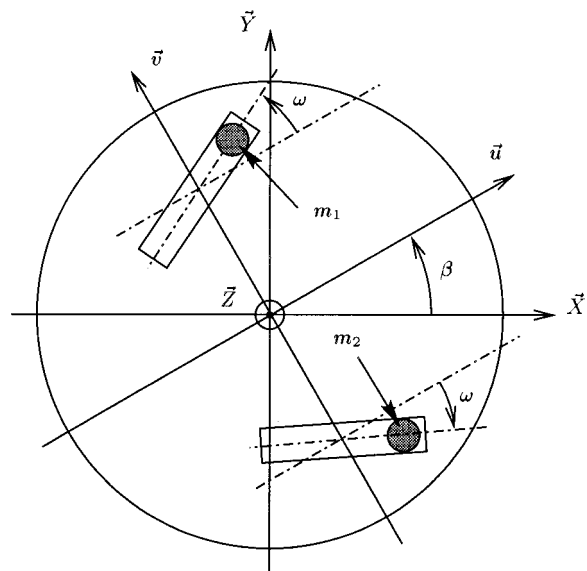


Fig. 3 Scheme of the vibration generator and definition of its parameters

them rotate synchronously in opposite directions. The excitation forces in the  $u$  and  $v$  directions are given by

$$F_u = (2\pi f)^2 r(m_1 + m_2) \cdot \cos(2\pi ft) \quad (5)$$

$$F_v = (2\pi f)^2 r(m_1 - m_2) \cdot \sin(2\pi ft). \quad (6)$$

Various motions of the tube are obtained by changing the excitation parameters such as the masses,  $m_1$  and  $m_2$ , the excitation frequency,  $f$ , the relative tube to support position,  $x$  and  $y$ , and the angular position of the vibration generator,  $\beta$ .

**3.2 Adjustment of the Finite Element Model.** As stated before, it is useful to take advantage of experimental values of modal parameters in the numerical model. In this section, the numerical parameters are adjusted on modal test in air and, partially, in water.

The modeling is identical to that presented in Phalippou and Delaune [7]. The wear test rig was modeled by beam finite elements (Fig. 4) with a bending stiffness,  $K_1$ , at the clamped end adjusted to  $10^4$  Nm/rad to match the predicted and measured frequencies and shapes of the first two modes in air (Fig. 5). The link between the generator and the excitation tube was also simulated by another bending stiffness,  $K_2$ , whose value was set to  $10^3$  Nm/rad in order to match the third numerical mode shape to the experimental data.

The impact stiffness,  $K_c$ , including ovalization and residual stiffness of modes, is taken as  $2.4 \cdot 10^6$  N/m. Thus, only the first six bending modes are required in each transverse direction to produce a good simulation. The retained modal characteristics in water are summarized in Table 1, where the damping ratios of the three highest modes were assumed equal to the third mode value. A comparison of computed and experimental linear vibratory analysis under forced excitation with different pairs of masses and several excitation frequencies showed that a correcting factor of 0.7 is needed in the expressions of the excitation forces (5) and (6) [7,16].

$$\begin{aligned} l_1 &= 551 \times 10^{-3} \text{ m} & E_1 &= 2.14 \times 10^{11} \text{ N/m}^2 & d_{4o} &= 14.2 \times 10^{-3} \text{ m} \\ l_2 &= 404 \times 10^{-3} \text{ m} & \rho_1 &= 8440 \text{ kg/m}^3 & E_4 &= E_2 \\ h_1 &= 25 \times 10^{-3} \text{ m} & d_{2o} &= 9.7 \times 10^{-3} \text{ m} & \rho_4 &= \rho_2 \\ h_2 &= 10 \times 10^{-3} \text{ m} & d_{2i} &= 8.75 \times 10^{-3} \text{ m} & d_{5o} &= 110 \times 10^{-3} \text{ m} \\ h_5 &= 59 \times 10^{-3} \text{ m} & E_2 &= 2 \times 10^{11} \text{ N/m}^2 & E_5 &= 7 \times 10^{10} \text{ N/m}^2 \\ d_{1o} &= 13.8 \times 10^{-3} \text{ m} & \rho_2 &= 7900 \text{ kg/m}^3 & \rho_5 &= 2700 \text{ kg/m}^3 \\ d_{1i} &= 9.5 \times 10^{-3} \text{ m} & d_{3i} &= 10.6 \times 10^{-3} \text{ m} & & \end{aligned}$$

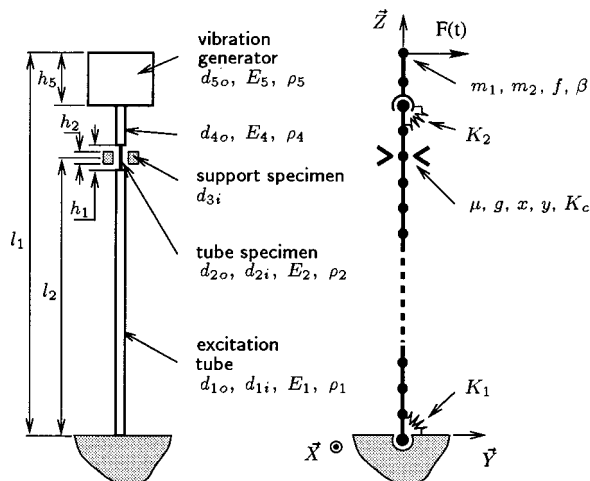


Fig. 4 Schematic diagram and modeling of the wear test rig

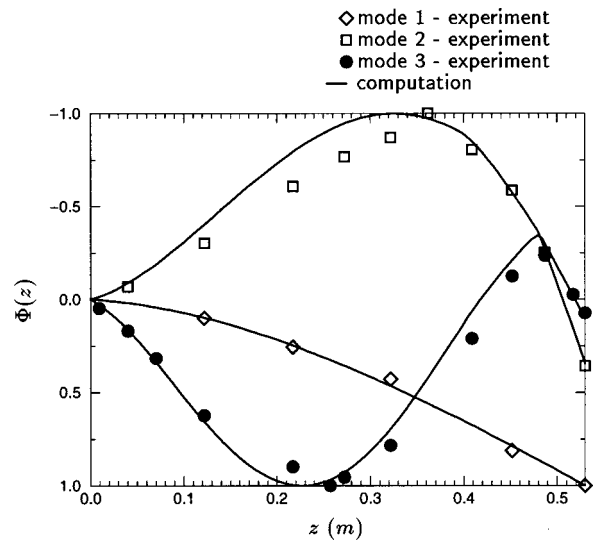


Fig. 5 Modal shape of the first three modes in air

Table 1 Modal characteristic in water

mode	$f_n$ (Hz)	$m_n$ (kg)	$k_n$ (N/m)	$\xi_n$ (%)
1	11.1	0.83	$4.04 \cdot 10^3$	0.37
2	96	0.45	$1.64 \cdot 10^5$	1.42
3	239	0.25	$5.64 \cdot 10^5$	1.5
4	500	0.22	$2.16 \cdot 10^6$	1.5
5	1010	0.17	$6.85 \cdot 10^6$	1.5
6	1780	0.16	$2.00 \cdot 10^7$	1.5

**3.3 Random Variables.** Among the set of parameters used in the modeling of a test on this wear machine, seven have been taken here as random variables. The sliding and static coefficients of friction,  $\mu_s$  and  $\mu_a$ , are rather difficult to assess and, as shown in Antunes et al. [11], Payen and de Langre [8] or Sauvé et al. [17], may have influence on the wear work rate. Moreover, by characterizing them randomly, one may account for possible changes during the wear test of the surface roughness and, thus, of the friction characteristics which are not controlled by the experimental apparatus. For our computation, we assumed they are identical ( $\mu = \mu_s = \mu_a$ ) and may vary between 0.15 and 0.30, based on Phalippou and Delaune [7]. The excitation frequency,  $f$ , was assumed to fluctuate by  $\pm 0.25$  Hz around the base value. This is the order of magnitude of typical frequency variations observed during tests on the vibration generator. The tube to support position, defined by  $x$  and  $y$ , and the generator angular position  $\beta$  also must be considered. We cannot ensure respectively a position better than 10 percent of radial clearance and  $\pm 10$  deg around the base value with the present apparatus. The diametral clearance,  $g$ , was assumed to vary in the range of the manufacturing tolerance of wear specimens.

A uniform distribution of the probability density function,  $p_i(X_i)$ , is used for the sake of simplicity [8,17] but it is not a restriction of the method. All other parameters are fixed in the sampling process.

**3.4 Simulation.** To illustrate the proposed approach, two different sets of excitation parameters are considered. The range of values used for each case is given in Table 2. It should be noted that the difference between the two cases concerns only the pair of masses, the range of excitation frequency and the generator angular position. For each computation, the simulated time is equal to

**Table 2 Excitation ranges of parameters of cases 1 and 2**

variable	case 1	case 2
$m_1$ (kg)	$8 \cdot 10^{-3}$	$5 \cdot 10^{-3}$
$m_2$ (kg)	$16 \cdot 10^{-3}$	$10 \cdot 10^{-3}$
$f$ (Hz)	[15.65, 16.15]	[14.65, 15.15]
$\beta$ ( $^\circ$ )	[35, 55]	[-10, 10]
$\mu$	[0.15, 0.30]	
$x$ (m)	[-0.045 $\cdot 10^{-3}$ , 0.045 $\cdot 10^{-3}$ ]	
$y$ (m)	[-0.045 $\cdot 10^{-3}$ , 0.045 $\cdot 10^{-3}$ ]	
$g$ (m)	[0.85 $\cdot 10^{-3}$ , 1 $\cdot 10^{-3}$ ]	

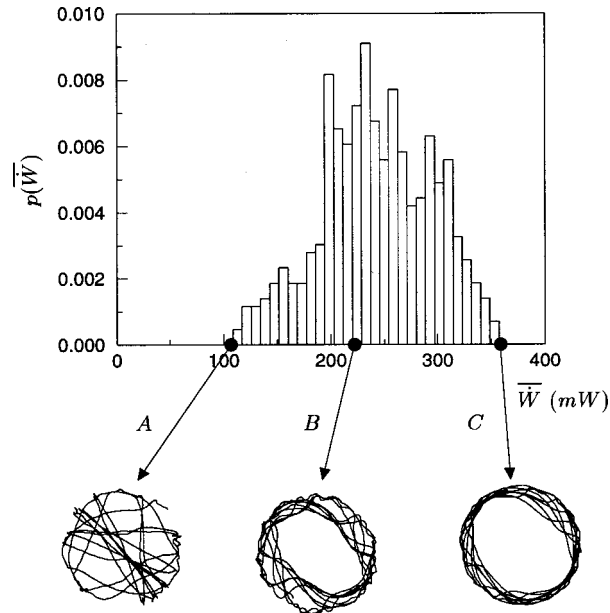


**Fig. 6 Probability density function of the mean wear work rate of case 1**

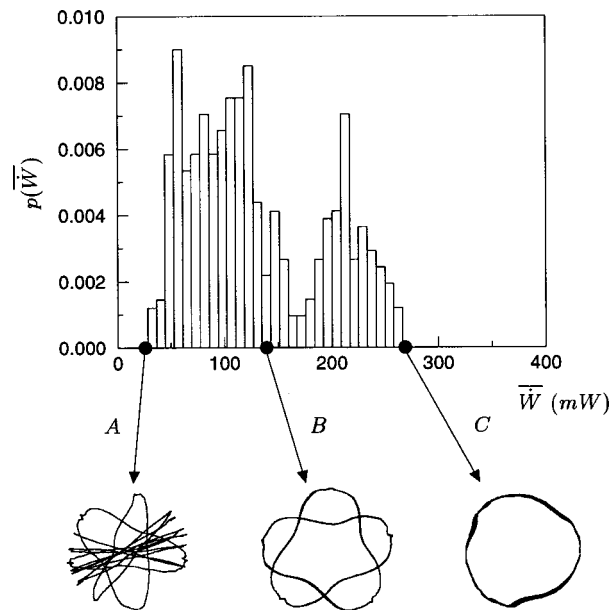


**Fig. 7 Probability density function of the mean wear work rate of case 2**

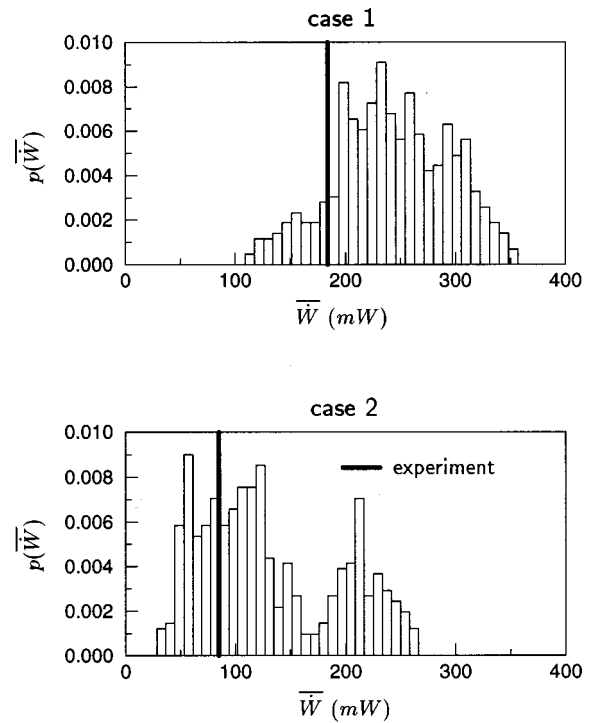


**Fig. 8 Comparison between experiment and simulation**

16 s but the mean wear work rate is calculated on the last 9 s in order to eliminate the transient response of the system (de Langre et al. [18]). The time step is  $3 \cdot 10^{-5}$  s. In their probabilistic computation, Payen and de Langre [8] have shown that a number of samples,  $M$ , equal to 1000 was sufficient to obtain good statistical accuracy. Sauvé et al. [17] also used 1000 samples in their recent work. For our application, some preliminary computations have shown that 400 samples were sufficient. This amounts to about 15 hours of CPU time on a IBM RS-6000 computer.

**3.5 Results.** For case 1, the probability density function of the mean wear work rate given by the Monte-Carlo simulations is presented in Fig. 6. One can note that this distribution is centered, and the ratio between the extreme values is about 3.5. Moreover,

	experiment	computation
case 1		
case 2		

**Fig. 9 Comparison of experimental and computed motions**

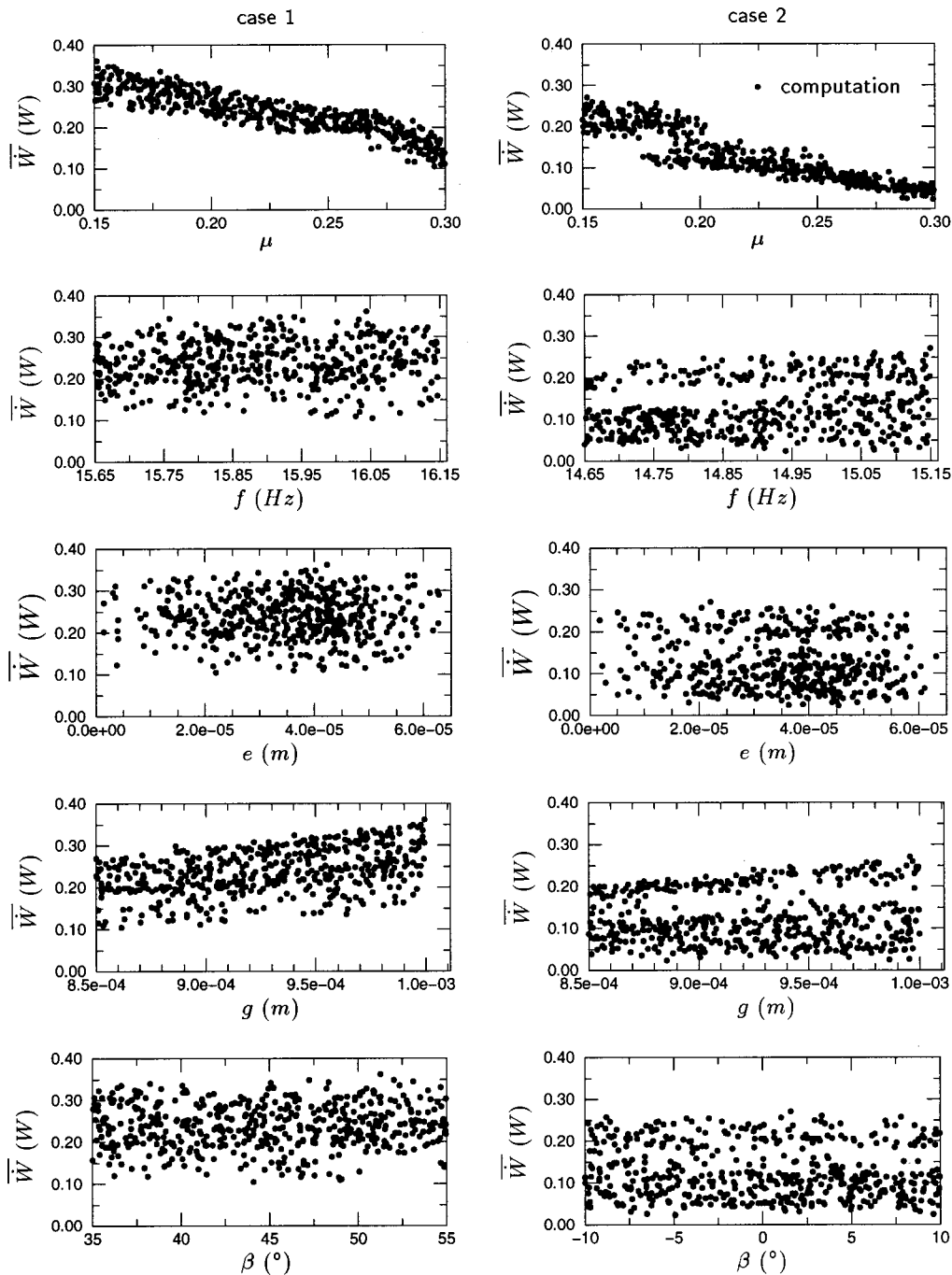


Fig. 10 Evolution of the mean wear work rate versus each random variable

the vibratory motions relating to the points *A*, *B*, and *C* are similar. This shows that the type of motion remains the same for each random configuration of the excitation conditions. This set of parameters may, thus, be considered as suitable.

For case 2 (Fig. 7), the pdf distribution is much more scattered and consists of two peaks separated by a region where the probability density is roughly zero. The dynamical motions related to points *A*, *B*, and *C* show that several types of motion may exist. The motion changes from impact-sliding for the random sample of point *A* to rubbing at point *C*, and the ratio of mean wear work rate between these two points is about 11. Consequently for this case, the simulation shows such excitation conditions may lead to unacceptable variations, and this set of parameters may be considered as unsuitable.

### 3.6 Comparison Between Experiment and Simulation

Two single tests were performed corresponding to the two cases predicted above. The measured mean wear work rate falls within the probability density function range (Fig. 8) for each case. The comparison of predicted and measured motion (Fig. 9), using the adequate parameters, confirms that we can rely on our simulations of the wear test on this machine.

### 3.7 Sensitivity Analysis.

To understand which parameters influence the dynamics of each wear test, a sensitivity analysis is performed. For that, a map of the mean wear work rate versus each input parameter has been constructed. The results of this analysis for each parameter chosen in our work and each case are presented in Fig. 10 and now commented.

In both cases, it should be noted that the friction coefficient,  $\mu$ , clearly has a significant effect on the mean wear work rate, which decreases when  $\mu$  increases. It is known that small values of  $\mu$  favor sliding which induces an increase of the wear work rate [11,8,17]. This is a general feature, but the quantitative influence of  $\mu$  on the wear work rate actually depends on the level and nature of the driving force and the other dynamical parameters. This is related to the nonlinear nature of the Coulomb law of friction. In Payen and de Langre [8], the wear work rate decreases of about one decade when  $\mu$  varies between 0 and 0.15, but is almost constant for higher values. In the present cases, Fig. 10, the wear work rate decreases on all the range of variation of  $\mu$ . This evolution is almost linear for case 1, but appears more erratic for case 2, when  $\mu$  varies between 0.18 and 0.2. For a given friction coefficient in this range, the mean wear work rate may vary by a factor of two indicating a change of vibratory regime, namely sliding to impact sliding.

The frequency of the driving force has here a negligible influence on the wear work rate for both cases. This is clearly the consequence of the very small range of variation we have considered here in constancy with experimental evidence.

To visualize the effect of the tube to support position, defined by  $x$  and  $y$  in our simulations, we use the resultant eccentricity parameter defined by  $e = \sqrt{x^2 + y^2}$ . In all cases, we observe that in the range of variability considered here, the tube to support position has no significant influence on mean wear work rate, so that no further refinement is needed in the test procedure on this parameter.

In both cases, the clearance,  $g$ , greatly affects the mean wear work rate. This might explain some of the scattering known in wear results for supposed similar tests, but in fact with different gaps. That also shows that the increase of gap due to wear may in some cases alter both the mean wear work rate and the vibratory regime.

The angular position of the excitation generator,  $\beta$ , has here no effect on the mean wear work rate in the range of variability considered in these two simulations.

## 4 Conclusion

Wear tests on simulators are generally used in the process of evaluating flow-induced wear of some components in pressurized water reactors. These tests are designed to measure a loss of volume associated to a value of mean wear work rate.

We proposed here a predictive probabilistic approach to the dynamics of these tests in order to help in the choice of the test parameters. With this method, sets of test parameters that would eventually lead to strong variations of vibratory regimes and wear work rate during the test may be detected beforehand. Thus expensive wear tests that would not be usable to derive accurate wear coefficients may be avoided.

This approach is then applied to a room temperature wear test rig and the results are compared with test data. A range of parameters unsuitable for wear tests is identified.

The proposed probabilistic computations also give statistical tendencies on the influence of each test parameter. In the particular applications considered here, friction and gap are shown to have a strong influence on wear work rate, while the driving force frequency or the specimen centering induce minor evolutions in their observed range of variations.

The proposed methodology is thought to be useful in the undertaking of long-duration high temperature wear tests by helping in the practical choice of test parameters.

## Acknowledgments

The work presented here was carried out as part of joint research and development program between the Commissariat à l'Énergie Atomique and the Electricité de France.

## Nomenclature

$a_n$	= modal damping
$e$	= eccentricity (m)
$f$	= excitation frequency (Hz)
$f_e^n, f_i^n$	= modal projection of the external and impact forces
$f_n$	= modal frequency (Hz)
$F_n$	= normal contact force (N)
$g$	= diametral tube-support gap (m)
$k$	= wear coefficient ( $\text{Pa}^{-1}$ )
$k_n$	= modal stiffness (N/m)
$K_c$	= impact stiffness (N/m)
$K_1$	= bending stiffness (Nm/rad)
$K_2$	= bending stiffness (Nm/rad)
$m_n$	= modal mass (kg)
$m_1, m_2$	= masses fixed on the vibration generator (kg)
$M$	= number of samples
$N$	= number of random variables
$p(\bar{W})$	= probability density function (pdf) of the mean wear work rate
$p_i(X_i)$	= pdf of the random variable $X_i$
$q_n, \dot{q}_n, \ddot{q}_n$	= generalized tube displacement, velocity, acceleration (m, $\text{ms}^{-1}$ , $\text{ms}^{-2}$ )
$r$	= gyration radius of masses $m_1$ and $m_2$ (m)
$\dot{V}$	= wear rate ( $\text{m}^3\text{s}^{-1}$ )
$\dot{W}$	= instantaneous wear work rate (W)
$\bar{W}$	= mean wear work rate (W)
$x, y$	= parameters of tube to support position (m)
$X_i$	= random variable
$X_t$	= tangential tube velocity ( $\text{ms}^{-1}$ )
$\beta$	= generator angular position ( $^\circ$ )
$\mu_a$	= static coefficient
$\mu_s$	= sliding coefficient
$\xi_n$	= modal damping ratio (percent) ( $= a_n/2\sqrt{k_n m_n}$ )
$\Phi_n$	= modal shape

## References

- [1] Paidoussis, M. P., 1979, "Flow-Induced Vibrations in Nuclear Reactors and Heat Exchangers," *Proceedings IAHR-IUTAM Symposium on Practical Experiences with Flow-Induced Vibrations*, Karlsruhe, Germany.
- [2] Pettigrew, M. J., and Campagna, A. O., 1979, "Heat Exchanger Tube Vibration: Comparison Between Operating Experiences and Vibration Analyses," *Proceedings IAHR-IUTAM Symposium on Practical Experiences with Flow-Induced Vibrations*, Karlsruhe, Germany.
- [3] Frick, T. M., Sobek, T. E., and Reavis, J. R., 1984, "Overview on the Development and Implementation of Methodologies to Compute Vibration and Wear of Steam Generator Tubes," *ASME Symposium on Flow Induced Vibration*, New Orleans, USA, **3**, pp. 149–161.
- [4] Archard, J. F., 1953, "Contact and Rubbing of Flat Surfaces," *J. Appl. Phys.*, **24**, pp. 981–988.
- [5] Fisher, N. J., Chow, A. B., and Weckwerth, M. K., 1994, "Experimental Fretting-Wear Studies of Steam Generator Materials," *ASME Symposium on Flow Induced Vibration*, Minneapolis, USA, PVP-273, pp. 241–255.
- [6] Ko, P. K., and Basista, H., 1984, "Correlation of Support Impact Force and Fretting-Wear for Heat Exchanger Tube," *ASME J. Pressure Vessel Technol.*, **106**, pp. 69–77.
- [7] Phalippou, C., and Delaune, X., 1996, "The Predictive Analysis of Wear Work-Rate in Wear Test Rig," *ASME Symposium on Flow Induced Vibration*, Montreal, Canada, PVP-328, pp. 247–256.
- [8] Payen, T., and de Langre, E., 1996, "A Probabilistic Approach for the Computation of Non-Linear Vibrations of Tubes Under Cross-Flow," *ASME Symposium on Flow Induced Vibration*, Montreal, Canada, PVP-328, pp. 337–346.
- [9] Rogers, R. J., and Pick, R. J., 1976, "On the Dynamic Spatial Response of a Heat Exchanger Tube with Intermittent Baffle Contacts," *Nucl. Eng. Des.*, **36**, pp. 81–90.
- [10] Axisa, F., Antunes, J., and Villard, B., 1988, "Overview of Numerical Methods for Predicting Flow Induced Vibrations," *ASME J. Pressure Vessel Technol.*, **110**, pp. 6–14.
- [11] Antunes, J., Axisa, F., Beaufils, B., and Guilbaud, D., 1990, "Coulomb Friction Modelling in Simulations of Vibration and Wear Work Rate of Multispan Tubes Bundles," *J. Flu. Struct.*, **4**, pp. 297–304.
- [12] Ko, P. K., 1979, "Experimental Studies of Tubes Frettings in Steam Generators and Heat Exchangers," *ASME J. Pressure Vessel Technol.*, **101**, pp. 125–133.

- [13] Ko, P. K., 1979, "Wear of Zirconium Alloys Due to Fretting and Periodic Impacting," *Wear*, **55**, pp. 369–384.
- [14] Ko, P. K., Tromp, J. H., and Weckwerth, M. K., 1982, "Heat Exchanger Tube Fretting-Wear: Correlation of Tube Motion and Wear," *ASME Material Evaluation Under Fretting Conditions*, ASTM STP 780, pp. 86–105.
- [15] Fisher, N. J., and Ingham, B., 1989, "Measurement of Tube-to-Support Dynamic Forces in Fretting-Wear Rigs," *ASME J. Pressure Vessel Technol.*, **111**, pp. 385–393.
- [16] Delaune, X., 1997, "Une Démarche Prédictive pour la Réalisation des Essais d'Usure par Impacts-Glislements," Ph.D. thesis, University Paris VI, France.
- [17] Sauvé, R. G., Morandin, G., and Savoia, D., 1997, "Probabilistic Methods for the Prediction of Damage in Process Equipment Tubes under Nonlinear Flow Induced Vibration," *ASME Symposium on Flow Induced Vibration*, Dallas, USA, AD-53-2, pp. 293–289.
- [18] Langre (de), E., Antunes, J., and Beaufils, B., 1991, "The Numerical Prediction of Vibrations in Tube Bundles Induced by Cross-Flow Turbulence," *Proceedings of the Fifth International Conference on Flow Induced Vibration*, Brighton, U.K., pp. 149–158.